Article

Effect of Capillary Number on the Residual Saturation of Colloidal Dispersions Stabilized by a Zwitterionic Surfactant

Han Am Son [1] and Taewoong Ahn [2,*]

[1] Department of Energy Resources Engineering, Pukyong National University, Busan 48547, Korea; hason@pknu.ac.kr
[2] Petroleum & Marine Research Division, Korea Institute of Geoscience and Mineral Resources, Daejeon 34132, Korea
* Correspondence: twahn@kigam.re.kr

Abstract: We investigated oil recovery from porous rock using nanoscale colloidal dispersions, formed by adsorption of an anionic polymer [poly-(4styrenesulfonic acid-co-maleic acid); PSS-*co*-MA] and a zwitterionic surfactant [*N*-tetradecyl-*N*, *N*-dimethyl-3-ammonio-1-propanesulfonate, TPS] onto silica nanoparticles. In an emulsion, colloidal dispersion enhanced the stability of the oil-water interface in the absence of particle aggregation; the hydrophobic alkyl chains of TPS shifted into the oil drop, not only physiochemically, stabilizing the oil-water interface, but also promoting repulsive particle-to-particle interaction. Core flooding experiments on residual oil saturation as a function of capillary number, at various injection rates and oil viscosities, showed that the residual oil level was reduced by almost half when the zwitterionic surfactant was present in the colloidal dispersion. Consequently, the result revealed that this colloidal dispersion at the interface provides a mechanically robust layer at the oil-water interface without particle aggregation. Thus, the dispersion readily entered the pore throat and adhered to the oil-water interface, lowering the interfacial tension and improving oil recovery.

Keywords: enhanced oil recovery; silica nanoparticles; capillary number; zwitterionic surfactant

1. Introduction

Colloidal dispersions using liquid suspensions of nanoparticles (NPs) have attracted considerable attention given their potential applications to enhanced oil recovery (EOR) from petroleum reservoirs [1–6]. NPs penetrate reservoir rocks; the particle diameter is less than 10% of that of the typical pore throat [7,8]. NPs are adsorbed by oil-water interfaces in rock pores [9–13]. In addition, mixing NPs with surfactants enhances NP surface activation [14–17]. For example, electrostatic adsorption of cationic surfactants onto silica NPs renders the particle surface hydrophobic; the silica particles move to the oil phase, further reducing the oil-water interface tension. In principle, adhesion energy is influenced by changes in NP interfacial tension and wettability, as expressed by $E = \pi R^2 \gamma_{ow}(1 - cos\theta)^2$, where E is the particle adhesion energy, R is the particle radius, γ_{ow} is the interfacial tension, and θ is the contact angle of the particle with the oil-water interface [18–20]. Surfactants change NP wettability; the oil droplet contact angle approaches 90°. The effect of wettability increases exponentially, thus raising the adhesion energy. For this reason, surface active nanoparticles can stabilize emulsions for mobility control in improved oil recovery processes, and small oil drops flow well through porous media [21].

However, colloidal NPs require some factors to be utilized in the reservoir. First, NPs should not aggregate, even under salinity conditions. The typical salinities of giant oil/gas reservoirs are 30 g/L (sandstone) and 90 g/L (carbonates) [22]. Under thes salinity conditions, electrostatic interactions between nanoscale particles are highly sensitive to ionic strength. At high ionic strengths, particles may readily aggregate because

of both reductions in the Debye length and electrostatic attractions between two oppositely charged molecules. If colloidal dispersions precipitate within reservoir rocks, fluidity is compromised because rock permeability decreases [23]. Recently, to increase applications in sandstone reservoirs with high salinity and high temperatures, SiO_2 NPs co-stabilized by a low-molecular-weight ligand (steric stabilization) and a zwitterionic surfactant (electrostatic stabilization) were developed [24]. However, these synthesis techniques are costly and time-consuming, because these methods can obtain only a very small amount of surface-modified NP at once and require many step by step processes. Thus, as the second factor to apply to the reservoir, a more efficient method is required for formation of colloidal dispersion.

Unlike conventional techniques for synthesis of colloidal dispersions, in this study, we homogeneously mixed anionic polymer with zwitterionic surfactant on the surface of silica nanoparticles in an applied shear stress manner using an ultrasonic homogenizer. Since this method can adsorb polymers and surfactants on the surface of nanoparticles via van der Waals attraction and dipole-charge interaction in a short time, it is very useful and realistic to produce many colloidal dispersions for reservoir applications. More specifically, this study evaluated electrostatic stabilization and particle aggregation at the oil-water interface using surfactants with different electrostatic properties, to enhance colloidal NPs/anionic polymer; of the two surfactants tested, one was cationic [dodecyltrimethylammonium bromide (DTAB)] and the other was zwitterionic (3-(*N*,*N*-dimethylmyristylammonio) propanesulfonate, TPS). Then, we also investigated how electrostatic stabilization of NPs affected flow within porous rocks such as core plugging phenomenon. Finally, we explored how the zwitterionic surfactant on NPs dispersions quantitatively affects residual oil saturation according to the capillary number, which is still insufficient in most previous studies. To investigate the effects of changes in residual oil saturation after adsorption of a zwitterionic surfactant, ultimate oil recovery and residual oil saturation were analyzed with and without the zwitterionic surfactant as a function of injected velocity of colloidal dispersions and oil viscosity.

2. Experimental

2.1. Materials

The oils used were *n*-dodecane (Kanto Chemical, Tokyo, Japan), KF-96-10 (Shinetsu, Tokyo, Japan), KF-96-100 (Shinetsu, Tokyo, Japan), and KF-96-500 (Shinetsu, Tokyo, Japan), with viscosities of about 1.3, 10, 100, and 500 cp, respectively. The colloidal hydrophilic silica solution was Ludox CL-X (45 wt% suspension in H_2O; particle diameter, 22 nm; purity, >99.8%; Sigma Aldrich, St. Louis, Mo, USA). An anionic polymer [the sodium salt of poly (4-styrenesulfonic acid-*co*-maleic acid); PSS-*co*-MA; 99% purity) was purchased from Sigma Aldrich, as were the two surfactants, i.e., the cationic dodecyl trimethylammonium bromide (DTAB) (99% pure) and zwitterionic *N*-tetradecyl-*N*,*N*-dimethyl-3-ammonio-1-propanesulfonate (TPS) (99% pure). We used Berea sandstone core (diameter, 3.8 cm; length, 5–6 cm) for the flow experiments. The brine porosity was 19.8–21.3%, and the brine permeability 138–154 md, when flooded.

2.2. Preparation of Colloidal Dispersions

The aqueous phase was a solution of Ludox CL-X (0.5 wt% particles) in NaCl (3 wt%). The anionic polymer PSS-*co*-MA was added to 0.5 wt% and mixed for 5 min using a magnetic stirrer operating at 800 rpm. Next, the zwitterionic surfactant TPS was added to 0.1 wt% followed by mixing for about 1 h and homogenization for 2 min (2 s on/1 s off) at 3000 rpm using an ultrasonic homogenizer (Digital Sonifier; Branson, MO, USA). Here, we determined the ratio of mixture after a stability test of phase behavior for colloidal dispersions.

2.3. Evaluation of Emulsification

Phase separation of four colloidal dispersions (8 mL samples in 10-mL glass bottles) was evaluated. To explore how cationic and zwitterionic surfactants affected colloidal dispersion, 0.1 wt% DTAB and 0.1 wt% TPS were added to dispersions containing 0.5 wt% PSS-*co*-MA and 0.5 wt% silica NPs in NaCl 3 wt%. Then, adding 10-cp oil into the colloidal dispersion while applying a mechanical stress at room temperature produced microscale emulsions. Phase separation of emulsion was examined after 12 h.

2.4. Core Flooding Experiments

The core flooding apparatus included an injection pump (500D syringe pump; Teledyne ISCO, Lincoln, NE, USA), an accumulator (CFR-100-100; TEMCO, Inc., Loveland, OH, USA),t a core holder (Young-sung Tech, Daejeon, Korea), and a measuring cylinder (Figure 1). The inflow line from the accumulator was connected to the core holder, which was packed with Berea sandstone. To prepare the initial state in sandstone, water was injected into the sandstone, followed by oil into the water-saturated sandstone until no more water was produced. The initial sandstone water and oil volume fractions were calculated by reference to the amount of water exuded. In the core flooding experiments, the complex colloidal dispersion fluid (mixed with silica, PSS-*co*-MA polymer, and TPS) was injected into the core holder via the accumulator at a constant flow rate of 1~10 mL min^{-1}, corresponding to a Darcy velocity of 4.1~41.0 ft day^{-1}. The fluid that flowed through the sandstone was collected in a measuring cylinder. Oil recovery was calculated by reference to the amount of oil extracted from the sandstone. Pressure transducers (DXD; Heise, Stratford, CT, USA) were installed at the inlet and outlet of the core holder to monitor pressure changes. To avoid any effect of NP thermal motion, all experiments were performed at 25 °C.
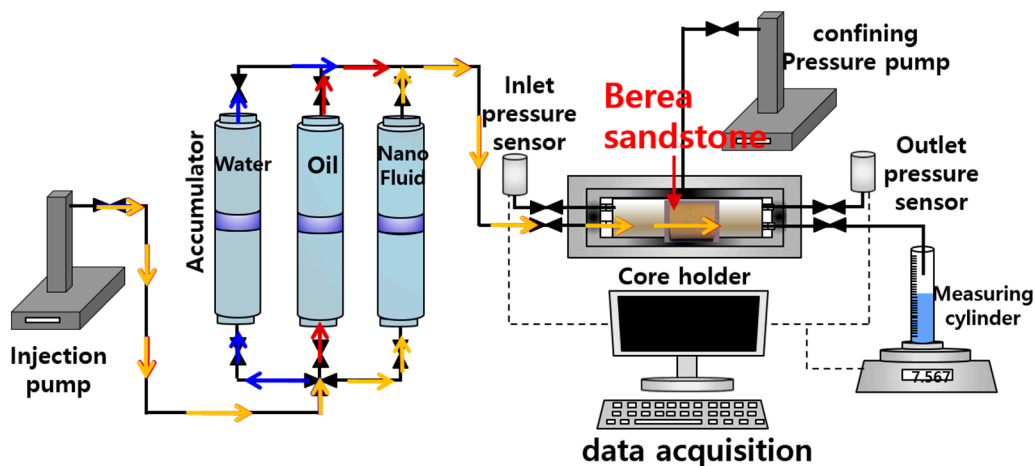

Figure 1. Schematic of the core flooding apparatus used to evaluate oil recovery.

3. Results and Discussion

3.1. Dispersion Properties of Silica NPs at the Oil-Water Interface

To explore whether surfactants differing in electrostatic properties affected silica NP suspensions at the oil-water interface, we added DTAB (a cationic surfactant) or TPS (a zwitterionic surfactant) with PSS-*co*-MA adsorbed onto the NPs and evaluated the phase behaviors of the emulsions. The bare silica NPs used in the experiment for emulsion formation had average diameters of ~22 nm showing a spherical shape from the TEM analysis (Figure 2). As shown in Figure 3, both silica NPs alone (sample 1) and PSS-*co*-MA combined with NPs (sample 4) exhibited unstable suspension properties at oil-water interfaces; the oil phase separated from the emulsion after 12 h (samples 1 and 4).

Theoretically, PSS-*co*-MA (an anionic polymer) should effectively adsorb to silica NPs while rendering more negative charges on the particle surface via protonation of sulfonic and carboxylic groups, thus improving NP aqueous suspension stability by enhancing electrostatic repulsion [25]. However, phase stability was clearly inadequate; silica NPs rather locate into water phase than the oil-water interface because silica particles at the interface remained wholly hydrophilic. After adsorption of hydrophobic DTAB (sample 2) or TPS (sample 3) onto the surfaces of otherwise naked silica NPs, their wettability at the oil-water interface changed. Nevertheless, a gel phase was evident after 12 h, reflecting strong electrostatic particle-particle attraction under highly saline conditions. Likewise, when cationic DTAB was added to NPs adsorbed by PSS-*co*-MA (sample 5), the negative charges of the NPs were neutralized, thereby weakening electrostatic repulsion. Thus, the NPs aggregated at the oil-water interface and the emulsion changed to a gel. However, absorption of the zwitterionic surfactant to NPs adsorbed with PSS-*co*-MA (sample 6) enhanced oil-water interface stability in the absence of NP aggregation, because the hydrophobic alkyl chains of TPS oriented into the oil drop (sample 6). In sample 6, the adsorption of PSS-*co*-MA on silica NPs was possibly generated by van der Waals attraction. Furthermore, adsorption of zwitterionic surfactant onto NPs is mediated by dipole-charge interaction between the trimethylammonium groups of zwitterionic surfactant and negatively charged particles with PSS-*co*-MA under brine as shown in Figure 4 [26].
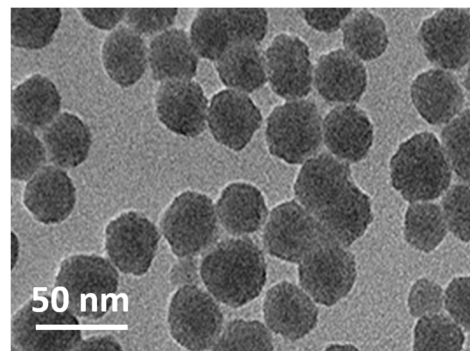
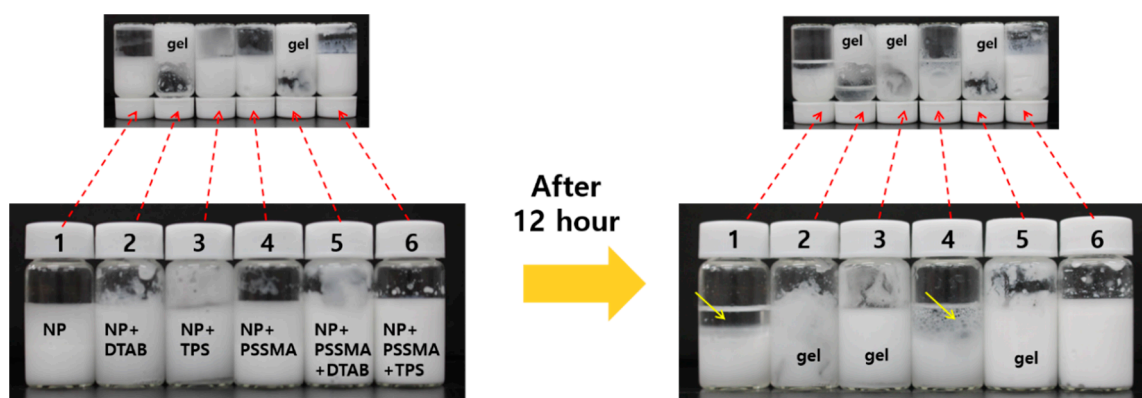

Figure 2. TEM image of silica nanoparticle.

Figure 3. Emulsion stabilities of various colloidal dispersions. In samples 1 and 4, a yellow arrow indicates the oil due to phase separation.
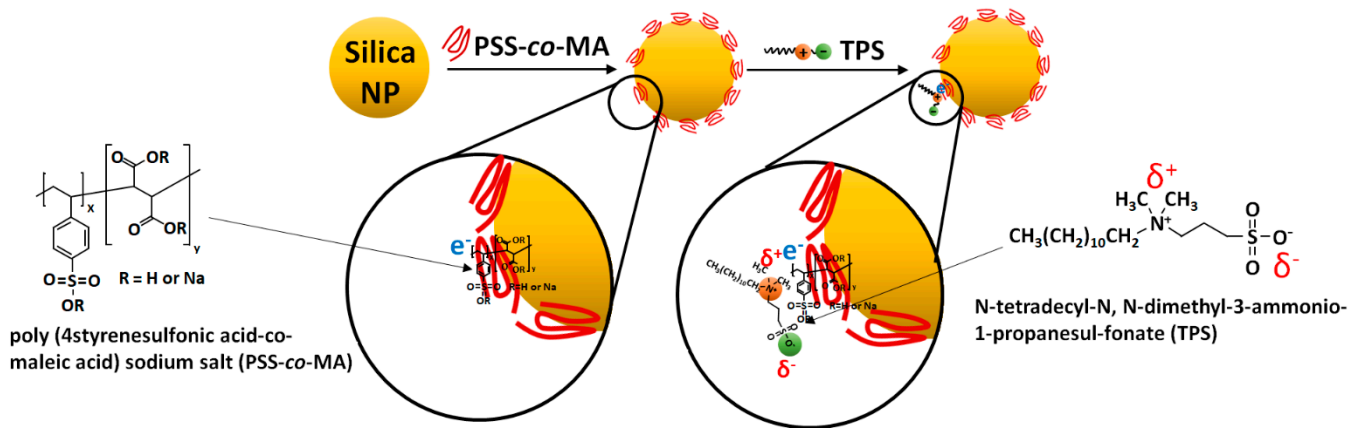
Figure 4. Schematic diagram of adsorption of zwitterionic surfactant onto negatively charged silica nanoparticle with PSS-*co*-MA.

We experimentally confirm that the ζ potential values are varied depending upon by adsorption of surfactants and polymers on the silica NPs (Figure 5). The ζ potential values of NPs used for samples 2, 3, and 5 (gel state) were more neutral than those for samples 1, 4, and 6 (emulsion state). It was confirmed that the ζ potential should be approximately less than -40 mV to maintain the emulsion state without aggregation of NPs at the oil-water interface.
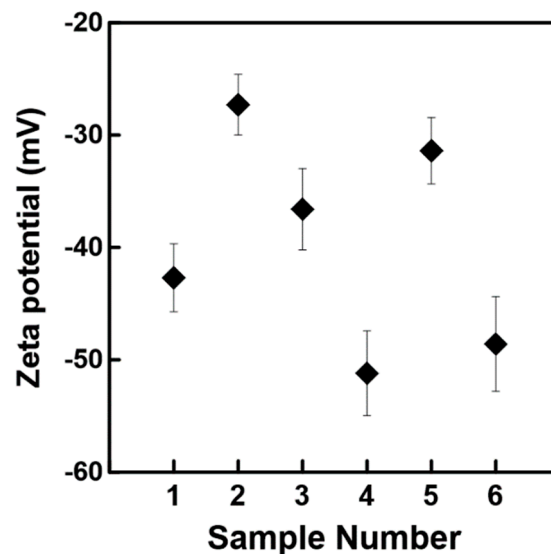

Figure 5. Zeta potential measurement of samples 1–6 in Figure 3.

3.2. Plugging of Porous Rock by Aggregates of Colloidal Dispersions

To investigate plugging of porous rock by particle aggregates, we performed two core flooding experiments; we injected NP/PSS-*co*-MA colloidal dispersions combined with the zwitterionic (TPS) or cationic (DTAB) surfactant. NP dispersions that included the zwitterionic surfactant exhibited a strong electrostatic repulsive force during core flooding, associated with high injectivity (0.13 mL/psi) and high-level oil recovery (74.2%) (Figure 6a). On the contrary, when colloidal dispersions with the cationic surfactant were injected, they gelled (aggregated) at the sandstone core inlets, thereby plugging the porous rock (Figure 6b). Injection of colloidal dispersions containing the zwitterionic surfactant was therefore optimal.
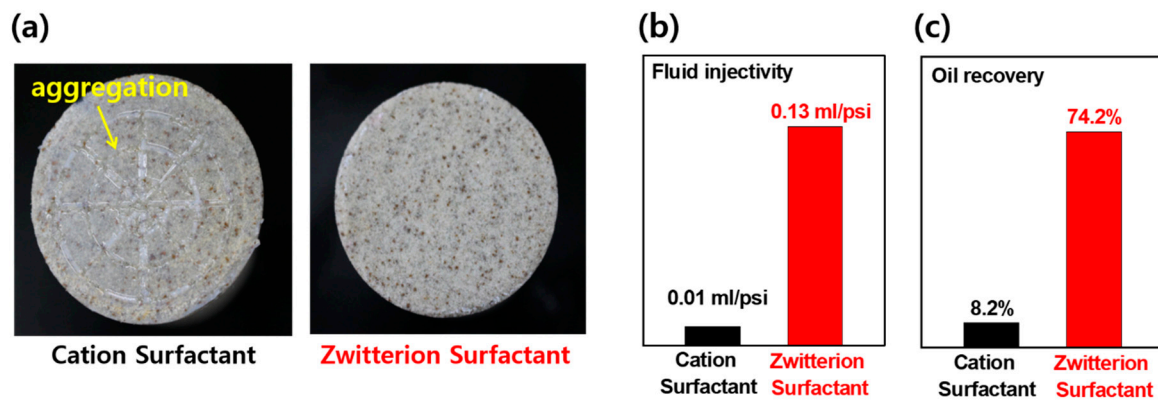
Figure 6. (**a**) Particle aggregation at sandstone inlets on injection of colloidal dispersions containing a cationic surfactant. Reduced (**b**) fluid injectivity and (**c**) oil recovery attributable to aggregation.

3.3. Effect of Flow Rate on Oil Production with Injection of Colloidal Dispersions

We confirmed that injection of colloidal dispersions containing a zwitterionic surfactant on silica NPs adsorbed by PSS-*co*-MA significantly increased the flow rate and oil recovery from Berea sandstone (Figure 7a). A possible explanation for this result is that the elevated flow velocity detached the NPs from rock, due to the increased hydrodynamic force; the NPs then readily adsorbed to oil-water interfaces, thus improving oil recovery. Indeed, NP retention fell as the flow rate increased, and the normalized breakthrough NP level rose (Figure 7a). We calculated the relative permeability of the oil-water phase, to characterize fluid flow by flow rate, using both the Corey correlation and our experimental data. The relative permeability is calculated as follows: $k_{ro} = k^0_{ro} \left(\frac{S_0 - S_{0r}}{1 - S_{wir} - S_{or}} \right)^m$, $k_{rw} = k^0_{rw} \left(\frac{S_w - S_{wir}}{1 - S_{wir} - S_{or}} \right)^n$ where k_{ro} and k_{rw} are the relative permeabilities of oil and water, respectively, S_{wir} is the irreducible (minimum) water saturation, and S_{or} is the (experimental) residual (minimum) oil saturation of porous rock. *m* and *n* are adjusted using a parameter estimation method (here, both values were 2). k^0_{ro} and k^0_{rw} are the relative permeabilities of oil and water, respectively, at the experimental endpoints (S_{wir} and S_{or}). As the colloidal dispersion flow rate increased, the residual oil saturation ($S_{or} = 1 - S_{w,\,max}$) fell and the relative water permeability at the endpoint (k^0_{rw}) increased; k^0_{rw} and S_{or} were 0.024 and 0.275, respectively, at a flow rate of 0.1 mL/min, but 0.203 and 0.177 at a flow rate of 10 mL/min (Figure 7b). Thus, silica NPs readily flowed through the pore throat, increasing water permeability when residual oil saturation was achieved.
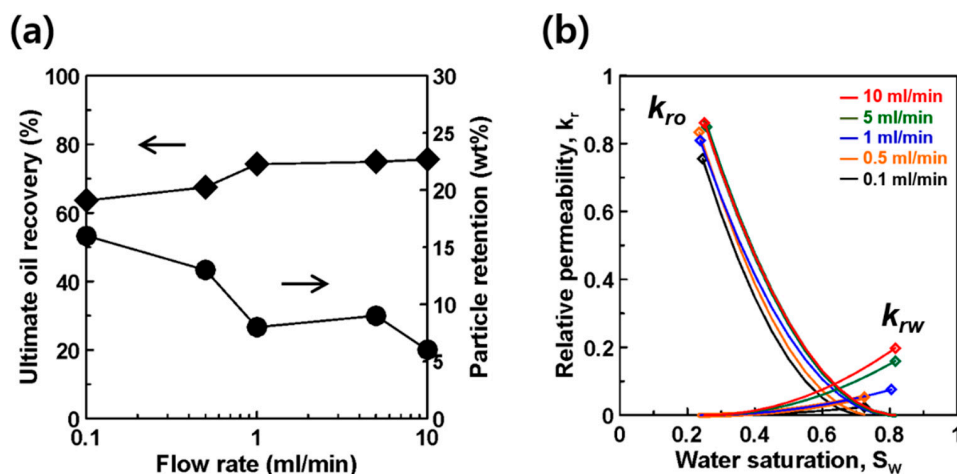

Figure 7. (**a**) Ultimate oil recovery and particle retention. (**b**) Relative permeability as a function of flow rate.

3.4. Effect of Oil Viscosity on Oil Production with Injection of Colloidal Dispersions

To evaluate how oil viscosity affected oil recovery from saturated reservoir rocks, we performed core flooding experiments using oils varying in viscosity. As viscosity increased recovery decreased, from 79.1% for a 1.3-cp oil to 57.8% for a 500-cp oil (Figure 8a). Thus, the viscosity difference between the colloidal dispersion (the water phase) and the displaced oil phase affected displacement efficiency. At the pore scale, when the shear stress at the pore throat increases, the residual oil flow velocity falls with increasing oil viscosity; colloidal dispersions readily bypass trapped residual oil. Oil viscosity also affected the oil-water relative permeability curves; the higher the viscosity of the residual oil, the lower the relative water permeability at the endpoint (Figure 8b), reflecting excessive viscous 'fingering' induced by formation of an unstable interface between the colloidal dispersion (the water phase) and oil. Furthermore, the fractional flow curves for oils of higher viscosity were much steeper than those for lower-viscosity oils, as explained by $f_w = \dfrac{1}{1+\left(\frac{k_{ro}}{k_{rw}}\right)\left(\frac{\mu_w}{\mu_o}\right)}$,

where f_w is the fractional flow of water, k_{ro} and k_{rw} are the relative permeabilities of oil and water, respectively, and μ_o and μ_w are the viscosities of oil and water, respectively. Thus, water breakthrough occurs at an early stage when oil viscosity is high (Figure 8c). The saturation points are shown as in Figure 8c; lines were drawn from the initial water saturation points tangential to the fractional flow curves. The arrows show the mean water saturation at the breakthrough points of the injection fluid (S_{wf}): the values ranged from ~0.44 (100-cp oil) to 0.76 (1.3-cp oil) and S_{wf} increased with decreasing oil viscosity. The fractional flow curves thus show that residual oil saturation decreased at higher oil viscosities because the flow bypassed the oil more easily.
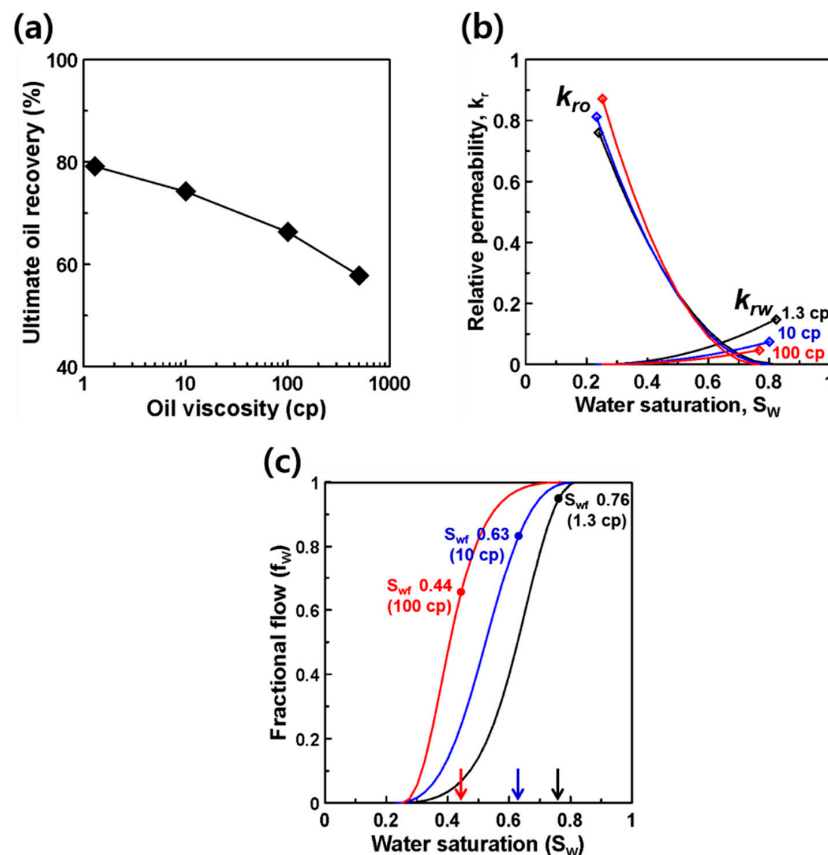

Figure 8. (**a**) Ultimate oil recoveries. (**b**) Relative permeabilities. (**c**) Fractional flow by oil viscosity. (S_{wf}: water saturation at injection fluid breakthrough. k_{ro} and k_{rw} are the relative permeabilities of oil and water, respectively).

3.5. Changes in Residual Oil Saturation after Adsorption of a Zwitterionic Surfactant

To determine whether oil recovery was enhanced via adsorption of a zwitterionic surfactant to PSS-*co*-MA adsorbed onto nanoscale colloidal dispersions, we analyzed ultimate oil recovery as a function of flow rate and oil viscosity. Colloidal dispersions with the zwitterionic surfactant produced more oil than dispersions without surfactant. In particular, oil recovery at an injection rate of 10 mL/min was higher than that at an injection rate of 0.1 mL/min (Figure 9a). The recovery of 10-cp oil was greater than that of 500-cp oil (Figure 9b). Thus, addition of a zwitterionic surfactant to the colloidal dispersion was advantageous. We explored the stability of Pickering emulsions with and without the zwitterionic surfactant as a function of oil viscosity. As shown in Figure 9c, the preparation containing the zwitterionic surfactant exhibited excellent emulsifying efficiency. In contrast, samples without surfactant exhibited phase separation; the colloidal dispersion adsorbed poorly to the oil-water interface. Thus, zwitterionic surfactant led to EOR; TPS reduced the interfacial tension from 44.1 to 8.7 mN/m from measurement result.
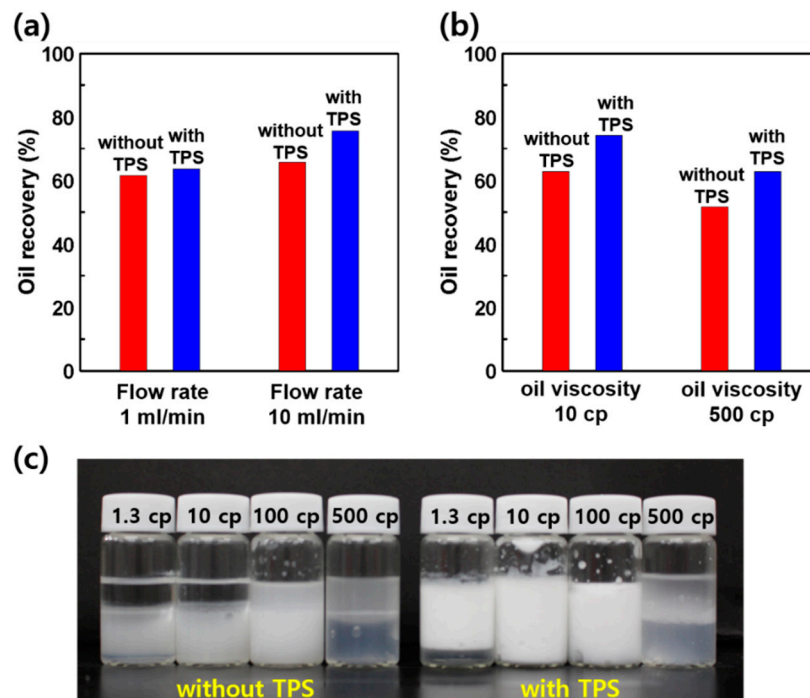

Figure 9. Oil recovery as a function of (**a**) flow rate and (**b**) oil viscosity in the presence or absence of a zwitterionic surfactant. (**c**) Emulsion stability as a function of oil viscosity in the presence or absence of a zwitterionic surfactant.

To explore the effects of viscous and capillary forces on residual oil saturation, we calculated saturation by capillary number (N_c) (Figure 10) using $N_c = \frac{v\mu_w}{\sigma_{ow}}$, where v is the interstitial velocity, μ_w is the viscosity of the colloidal dispersion, and σ_{ow} is the interfacial tension between the oil phase and the dispersion. The capillary number depends on the injection rate and oil viscosity. As shown in Figure 10, residual oil saturation decreased with increasing capillary number. In general, capillary forces are negligible compared to viscous forces when the capillary number is higher than 10^{-5}; oil recovery is dominated by the viscous force. We found that a colloidal dispersion containing a zwitterionic surfactant reduced the residual oil in rock by more than 10%, versus 5% without the surfactant. The zwitterionic led to EOR. These results highlight that the zwitterionic TPS surfactant used in colloidal dispersions would display the sufficient reduction of residual oil saturation without particles aggregation in porous rock under salinity conditions.
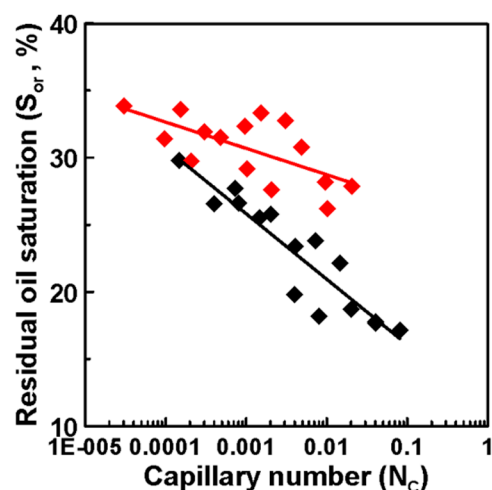
Figure 10. Residual oil saturation as a function of capillary number in the presence or absence of a zwitterionic surfactant (red: no surfactant; black: with surfactant).

4. Conclusions

We explored whether the addition of a zwitterionic surfactant to a colloidal dispersion affected oil recovery from porous rock. NPs were co-stabilized by surfactants; we hybridized an anionic polymer (PSS-*co*-MA) to a zwitterionic surfactant (TPS) on the surfaces of silica NPs. The adsorption of PSS-*co*-MA on silica NPs was possibly generated via van der Waals attraction. In addition, adsorption of zwitterionic surfactant onto NPs is mediated by dipole-charge interaction between the trimethylammonium groups of zwitterionic surfactant and negatively charged particles with PSS-*co*-MA under brine.

Core flooding experiments showed that colloidal dispersions with the zwitterionic surfactant prevented NP aggregation due to repulsive particle-to-particle interaction, unlike colloidal dispersions with a cationic surfactant. Thus, the dispersion readily entered the pore throat and adhered to the oil-water interface, lowering the interfacial tension and improving oil recovery. Regarding residual oil saturation as a function of capillary number, colloidal dispersion containing a zwitterionic surfactant reduced the residual oil level to half that noted in the absence of the surfactant; interfacial tension was significantly reduced. Therefore, our nanoscale colloidal dispersion led to EOR.

References

1. Ju, B.; Fan, T. Experimental study and mathematical model of nanoparticle transport in porous media. *Powder Technol.* **2009**, *192*, 195–202. [CrossRef]
2. Metin, C.O.; Bonnecaze, R.; Nguyen, Q. The viscosity of silica nanoparticle dispersions in permeable media. *SPE Reserv. Eval. Eng.* **2013**, *16*, 327–332. [CrossRef]
3. Maghzi, A.; Kharrat, R.; Mohebbi, A.; Ghazanfari, M.H. The impact of silica nanoparticles on the performance of polymer solution in presence of salts in polymer flooding for heavy oil recovery. *Fuel* **2014**, *123*, 123–132. [CrossRef]
4. Zhang, H.; Nikolov, A.; Wasan, D. Enhanced oil recovery (EOR) using nanoparticle dispersions: Underlying mechanism and imbibition experiments. *Energy Fuels* **2014**, *28*, 3002–3009. [CrossRef]
5. Roustaei, A.; Bagherzadeh, H. Experimental investigation of SiO2 nanoparticles on enhanced oil recovery of carbonate reservoirs. *J. Pet. Explor. Prod. Technol.* **2015**, *5*, 27–33. [CrossRef]
6. Yu, H.; He, Y.; Li, P.; Li, S.; Zhang, T.; Rodriguez-Pin, E.; Du, S.; Wang, C.; Cheng, S.; Bielawski, C.W. Flow enhancement of water based nanoparticle dispersion through microscale sedimentary rocks. *Sci. Rep.* **2015**, *5*, 8702–8709. [CrossRef]
7. Wyss, H.M.; Blair, D.L.; Morris, J.F.; Stone, H.A.; Weitz, D.A. Mechanism for clogging of microchannels. *Phys. Rev. E* **2006**, *74*, 061402. [CrossRef] [PubMed]
8. Zhang, T.; Murphy, M.J.; Yu, H.; Bagaria, H.G.; Yoon, K.Y.; Nielson, B.M.; Bielawski, C.W.; Johnston, K.P.; Huh, C.; Bryant, S.L. Investigation of nanoparticle adsorption during transport in porous media. *SPE J.* **2015**, *20*, 667–677. [CrossRef]
9. Hendraningrat, L.; Li, S.; Torsæter, O. A coreflood investigation of nanofluid enhanced oil recovery. *J. Pet. Sci. Eng.* **2013**, *111*, 128–138. [CrossRef]
10. Lu, T.; Li, Z.; Zhou, Y.; Zhang, C. Enhanced oil recovery of low-permeability cores by SiO$_2$ nanofluid. *Energy Fuels* **2017**, *31*, 5612–5621. [CrossRef]
11. Cheraghian, G.; Kiani, S.; Nassar, N.N.; Alexander, S.; Barron, A.R. Silica nanoparticle enhancement in the efficiency of surfactant flooding of heavy oil in a glass micromodel. *Ind. Eng. Chem. Res.* **2017**, *56*, 8528–8534. [CrossRef]
12. Li, Y.; Dai, C.; Zhou, H.; Wang, X.; Lv, W.; Zhao, M. Investigation of spontaneous imbibition by using a surfactant-free active silica water-based nanofluid for enhanced oil recovery. *Energy Fuels* **2018**, *32*, 287–293. [CrossRef]
13. Ali, J.A.; Kolo, K.; Manshad, A.K.; Stephen, K.D. Low-salinity polymeric nanofluid-enhanced oil recovery using green polymer-coated ZnO/SiO$_2$ nanocomposites in the upper Qamchuqa formation in Kurdistan region, Iraq. *Energy Fuels* **2019**, *33*, 927–937. [CrossRef]
14. Binks, B.P.; Rodrigues, J.A. Enhanced stabilization of emulsions due to surfactant-induced nanoparticle flocculation. *Langmuir* **2007**, *23*, 7436–7439. [CrossRef]
15. Binks, B.P.; Kirkland, M.; Rodrigues, J.A. Origin of stabilization of aqueous foams in nanoparticle−surfactant mixtures. *Soft Matter* **2008**, *4*, 2373–2382. [CrossRef]
16. Maestro, A.; Guzman, E.; Santini, E.; Ravera, F.; Liggieri, L.; Ortegaa, F.; Rubio, R.G. Wettability of silica nanoparticle–surfactant nanocomposite interfacial layers. *Soft Matter* **2012**, *8*, 837–843. [CrossRef]
17. Agista, M.N.; Guo, K.; Yu, Z. A state of the art review of nanoparticles application in petroleum with a focus on enhanced oil recovery. *Appl. Sci.* **2018**, *8*, 871. [CrossRef]
18. Binks, B.P. Particles as surfactants similarities and differences. *Curr. Opin. Colloid Interface Sci.* **2002**, *7*, 21–41. [CrossRef]
19. Aveyard, R.; Binks, B.P.; Clint, J.H. Emulsions stabilized solely by colloidal particles. *Adv. Colloid Interface Sci.* **2003**, *100*, 503–546. [CrossRef]
20. Fan, H.; Striolo, A. Nanoparticle effects on the water-oil interfacial tension. *Phys. Rev. E* **2012**, *86*, 051610. [CrossRef]
21. Zhang, T.; Davidson, D.; Bryant, S.L.; Huh, C. Nanoparticle-stabilized emulsions for applications in enhanced oil recovery. In Proceedings of the SPE Improved Oil Recovery Symposium, Tulsa, OK, USA, 24–28 April 2010; Society of Petroleum Engineers: Richardson, TX, USA, 2010.
22. Oruwori, A.E.; Ikiensikimama, S.S. Determination of water salinities in hydrocarbon bearing reservoirs of some Niger delta fields–Nigeria. In Proceedings of the Nigeria Annual International Conference and Exhibition, Calabar, Nigeria, 31 July–7 August 2010; Society of Petroleum Engineers: Richardson, TX, USA, 2010.
23. Kim, I.; Taghavy, A.; DiCarlo, D.; Huh, C. Aggregation of silica nanoparticles and its impact on particle mobility under high-salinity conditions. *J. Pet. Sci. Eng.* **2015**, *133*, 376–383. [CrossRef]
24. Zhong, X.; Li, C.; Li, Y.; Pu, H.; Zhou, Y.; Zhao, J.X. Enhanced oil recovery in high salinity and elevated temperature conditions with a zwitterionic surfactant and silica nanoparticles acting in synergy. *Energy Fuels* **2020**, *34*, 2893–2902. [CrossRef]
25. Tjipto, E.; Quinn, J.F.; Caruso, F. Assembly of multilayer films from polyelectrolytes containing weak and strong acid moieties. *Langmuir* **2005**, *21*, 8785–8792. [CrossRef] [PubMed]
26. Lin, W.; Kampf, N.; Klein, J. Designer nanoparticles as robust superlubrication vectors. *ACS Nano* **2020**, *14*, 7008–7017. [CrossRef] [PubMed]